Localization of Phospholipase A₂ in Normal and *ras*-Transformed Cells

Dafna Bar-Sagi,* Joseph P. Suhan,* Frank McCormick,‡ and James R. Feramisco*

*Cold Spring Harbor Laboratory, Cold Spring Harbor, New York 11724; and ‡Department of Molecular Biology, Cetus Corporation, Emeryville, California 94608

Abstract. The cellular localization of phospholipase A₂ (PLA₂) was examined in normal and *ras*-transformed rat fibroblasts using immunohistochemical techniques. Polyclonal antibodies were generated against porcine pancreatic PLA₂ and were affinity purified for use in this study. The antibodies detected a 16-kD band on immunoblots of total cellular proteins from fibroblasts. In cell-free assays of phospholipase A₂ activity, the purified antibodies inhibited the bulk of the enzyme activity whereas control IgG preparations had no effect. Immunofluorescence microscopy indicated that PLA₂ was diffusely distributed throughout the cell. Increased concentration of PLA₂ was de-

tected under membrane ruffles in normal and *ras*-transformed cells. Specific immunofluorescence staining was also detected on the outer surface of the normal cells. Immunoelectron microscopy demonstrated the increased accumulation of PLA₂ in membrane ruffles and also revealed the presence of the enzyme in microvilli and its association with intracellular vesicles. Ultrastructural localization of PLA₂ and the *ras* oncogene protein, using a double immunogold labeling technique, indicated a spatial proximity between PLA₂ and *ras* proteins in the ruffles of *ras*-transformed cells. The possible role of PLA₂ in the structural rearrangements that underlie membrane ruffling is discussed.

PHOSPHOLIPASE A₂ (PLA₂)[1] is a calcium-requiring esterase catalyzing the hydrolysis of fatty acid ester bonds specifically at the *sn*-2 position of glycerophospholipids (for review, see Van den Bosch, 1980). The Ca^{2+}-dependent phospholipases A₂ occurring in mammalian tissues are classified into two groups in terms of their localization. Extracellular PLA₂ which is abundant in pancreatic tissue, is synthesized in the form of an inactive proenzyme and is secreted into the pancreatic duct where it is converted into the active enzyme by tryptic removal of a heptapeptide from the NH₂-terminus of the molecule (de Haas et al., 1968). Pancreatic phospholipase A₂ has been studied extensively with respect to its physical and chemical characteristics (Verheij et al., 1981). The enzyme is a compact protein of ∼14 kD, stabilized by seven disulfide bridges. The production of secretory PLA₂ in the pancreas serves a digestive function. The intracellular phospholipase A₂, called hereafter PLA₂, has been characterized to a much lesser extent than the pancreatic enzyme because of its low cellular content and low specific activity.

The activity of PLA₂ has been postulated to play an important regulatory role in several metabolic pathways. For example, PLA₂ catalyzes the release of arachidonic acid which is the first and rate-limiting precursor in the biosynthesis of prostaglandins (Land, 1979). In addition, the activity of the enzyme is part of the phosphoglyceride deacylation-reacylation cycle and as such mediates the rapid metabolic turnover of membrane phospholipids. Receptor-controlled

activation of PLA₂ has been shown to accompany the stimulation of neutrophils by chemotactic peptide (Bormann et al., 1984), the activation of platelets by thrombin (McKean et al., 1981), the antigenic stimulation of mast cells (Siraganian, 1983), and the activation of chondrocytes by interleukin-1 (Chang et al., 1986). Furthermore, activation of PLA₂ has been implicated in the generation of receptor-mediated mitogenic signals. The proliferative response of Swiss 3T3 cells to PDGF (Shier and Durkin, 1982) and of thymocytes to interleukin-1 (Dinarello et al., 1983) appears to be mediated, at least in part, by PLA₂ stimulation and prostaglandin production. In addition, PLA₂ seems to be an important component of the mechanism by which mitogens activate Na^+/H^+ exchange (Vicentini et al., 1984). Finally, we have found recently that microinjection of the *ras*-oncogene protein into quiescent rat embryo fibroblasts induces an enhancement of PLA₂ activity (Bar-Sagi and Feramisco, 1986).

In spite of these important roles ascribed to the intracellular PLA₂, very little is known about the mechanisms that regulate the activity of the enzyme. To investigate the properties of cellular PLA₂, we have generated monospecific antibodies to PLA₂. In the present study we have used these antibodies to characterize the intracellular distribution of PLA₂ in normal and *ras*-transformed fibroblasts.

Materials and Methods

Antibodies

Preparation of Anti–PLA₂ Antibody. Homogeneous preparations of porcine pancreatic PLA₂ (Boehringer Mannheim Biochemicals, Indianapolis,

---

1. *Abbreviation used in this paper*: PLA₂, phospholipase A₂.

1649

IN) were used as immunogen for raising antibodies in rabbits. A mixture of native and SDS-denatured PLA₂ was injected subcutaneously according to the following schedule: 50 μg of PLA₂ in Freunds' complete adjuvant on day 0, 100 μg of PLA₂ in Freunds' incomplete adjuvant at 10-d intervals over a 2-mo period, and 100 μg booster injection in Freunds' incomplete adjuvant every 4–5 wk. Animals were bled at 1-mo intervals after the sixth injection. For the affinity purification of the antisera, 10 mg of PLA₂ were coupled to 1 ml of Affi-Gel 10 (Bio-Rad, Richmond, CA) by the manufacturer's recommended procedure. The coupling efficiency was >90%. The PLA₂ affinity column was prewashed with 75 mM Hepes (pH 7.5). The antisera were passed through the column three times and the column was then washed extensively with 75 mM Hepes (pH 7.5). Antibodies were eluted with 50 mM glycine HCl (pH 2.5) and the eluates were adjusted to neutral pH immediately by the addition of 0.5 M Tris-HCl (pH 7.5). The mouse monoclonal anti-*ras* antibody, 6B7, was prepared as described elsewhere (Wong et al., 1986). This antibody binds to both the protooncogenic and oncogenic forms of the *ras* protein (Wong et al., 1986). The rabbit polyclonal anti-Na,K-ATPase antibody, K2, was kindly provided by Dr. K. Sweadner (Harvard Medical School, Boston, MA). This antiserum was raised against the purified Na,K-ATPase from rat renal medulla (Sweadner and Gilkeson, 1985) and has been previously used for the specific localization of Na,K-ATPase by indirect immunofluorescence (McGrail and Sweadner, 1986).

Cell Culture

Normal rat kidney cells (NRK, CRL 1570) and Kirsten MSV-transformed rat kidney cells (KNRK, CRL 1569) were obtained from American Type Culture Collection (Rockville, MD). Cells were cultured in DME supplemented with 10% FCS (GIBCO, Grand Island, NY) and maintained at 37°C in a humid atmosphere containing 5% CO₂.

Electrophoresis and Immunoblotting

SDS-PAGE was performed essentially as described by Blattler et al. (1972) except that the buffer system of Laemmli (1970) was used. Proteins were transferred to nitrocellulose sheets by the blotting procedure described by Towbin et al. (1979). The nitrocellulose sheets were then incubated in a blocking solution (3% BSA in PBS) overnight, and then incubated for 2 h at 20°C with antibody solution (1:100 dilution of anti-PLA₂ antibody in 1% BSA in PBS). The sheets were rinsed three times for 5–10 min each in PBS, and then incubated in peroxidase conjugated goat anti-rabbit IgG (Bio-Rad, Richmond, CA) diluted 1:1,500 in 1% BSA in PBS for 1 h at 20°C. The sheets were again washed three times for 5–10 min each with PBS and then developed in 4-chloro-1-naphthol (3 mg/ml of 4-chloro-1-naphthol in methanol diluted with 5 vol of PBS to which 0.01 vol of 30% hydrogen peroxide was added).

Labeling of Phospholipids and Preparation of Cell Membranes for PLA₂ Assay

Subconfluent NRK cells were preincubated in phosphate-free DME supplemented with 5% phosphate-free FCS. After 1 h, carrier free ³²PO₄ was added to 100 μCi/ml for 2 h. At the end of the labeling period, cells were washed five times with phosphate-free DME and harvested in ice-cold hypotonic lysis buffer (20 mM Tris-HCl, pH 7.4, 10 mM NaCl, 0.1% 2-mercaptoethanol, 1% Aprotinin). After incubation for 20 min on ice, cells were ruptured with 40 strokes of a Dounce homogenizer. Cell lysates were sedimented at low speed (500 g for 5 min) to remove nuclei and the supernatant was centrifuged at 100,000 g for 30 min. The resulting membrane pellet was rinsed twice with incubation buffer (50 mM Tris-HCl, pH 8.0, 120 mM NaCl) and resuspended in incubation buffer for dispensing into reaction tubes. Calcium was omitted to inhibit the activity of PLA₂.

   Membranes from 10⁵–10⁶ cells were incubated in 100 μl reactions containing anti-PLA₂ IgG or control IgG (1:20 dilution of 1 mg/ml IgG preparation) at 4°C for 2 h. After this incubation period, reaction mixtures were supplemented with 5 mM CaCl₂ to trigger PLA₂ activity and then incubated at 37°C for the indicated intervals.

Phospholipid Analysis

Reactions were terminated by the addition of an ice-cold mixture of methanol, chloroform and HCl (2:1:0.02 vol/vol/vol) and phospholipids were extracted as described previously (Bar-Sagi and Feramisco, 1986). Chromatographic separation of phospholipids was carried out on silica gel LK6D TLC plates (Whatman Inc., Clifton, NJ) impregnated with 1% potassium

oxalate and activated for 15 min at 115°C, with the solvent system of chloroform, methanol, ammonia and water (45:30:3:5 vol/vol/vol/vol). The ³²P-labeled phospholipids were visualized by autoradiography and identified by co-chromatography with standards detected with iodine vapor.

Indirect Immunofluorescence

Cells plated on glass coverslips were washed twice with PBS and fixed at 20°C for 30 min in 3.7% formaldehyde in PBS. Coverslips were rinsed twice with PBS and cells were permeabilized by exposure to 0.2% Triton X-100 (Sigma Chemical Co., St. Louis, MO) in PBS for 30 s at 20°C. The affinity purified rabbit anti-PLA₂ antibody was used at a 1:50 dilution (20 μg/ml) in PBS containing 0.5 mg/ml BSA. The rabbit anti-Na,K-ATPase antiserum was used at a 1:400 dilution. Incubation with the primary antibody was for 1 h at 37°C in a humidified atmosphere. After two 10-min washes in PBS, cells were incubated with fluorescein-conjugated goat anti-rabbit antibody (Cappel Laboratories, Cochranville, PA) diluted 1:100 (10 μg/ml) in PBS containing 0.5 mg/ml BSA. Secondary antibody incubation was for 1 h at 37°C in a humidified atmosphere followed by two 10-min PBS washes, and a distilled water rinse before mounting with Gelvatol. Before use, the secondary antibodies were preadsorbed with methanol fixed NRK monolayers and clarified using a Beckman Airfuge. Cells were examined with a Zeiss photomicroscope III equipped for epifluorescence. Phase micrographs were recorded using Kodak Technical Pan film and fluorescence micrographs were recorded on Kodak Tri-X film.

Transmission Electron Microscopy

Cells were fixed for 30 min in a solution containing 2% glutaraldehyde, 75 mM cacodylate and 4.5% sucrose, pH 7.4. After several washes with 100 mM cacodylate buffer, the cells were post-fixed for 30 min in 1% osmium tetroxide in 75 mM cacodylate, pH 7.4. The cells were then washed several times with distilled water, en bloc stained for 30 min in saturated aqueous uranyl acetate and dehydrated in a graded series of ethanol followed by an overnight infiltration in 100% Epon. Fresh Epon was added the next day and polymerized for 24 h at 60°C. The Epon embedded cells were cut and stained with lead citrate. Electron micrographs were taken on a Philips 201 at 80kV.

Scanning Electron Microscopy

Cells were processed for scanning electron microscopy essentially as described above for transmission electron microscopy except that after ethanol dehydration the cells were critical-point dried using ethanol as a transitional solvent in a Bomar SPC 900EX. Dried specimens were mounted on stubs, sputter coated with gold, and observed in an Amray 1000 operated at 20 kV.

Immunoelectron Microscopy

Immunoperoxidase. Cells were grown on glass coverslips and fixed for 10 min in PBS buffered 2% paraformaldehyde at 25°C and transferred to 4°C for an additional 20 min. Cells were then washed with PBS and extracted for 30 s at 25°C with 0.1% Triton X-100 in PBS and again washed with PBS. The cells were incubated for 10 min in 50 mM NH₄Cl in PBS and washed for 10 min in PBS containing 1 mg/ml BSA (PBS/BSA). The primary antibody was diluted in PBS/BSA (affinity purified rabbit anti-PLA₂ antibody [20 μg/ml], mouse anti-*ras* antibody [10 μg/ml]) and the cells were incubated with the antibody for 1 h at 37°C. After incubation, the cells were washed for 1 h with several changes of PBS and then incubated for 1 h at 37°C with affinity-purified peroxidase-conjugated goat anti-mouse or goat anti-rabbit antibodies (Cappel Laboratories, Cochranville, PA) diluted 1:20 (50 μg/ml) in PBS/BSA. After an overnight wash with PBS at 4°C, the cells were fixed at 25°C for 5 min in 100 mM cacodylate buffered 2% glutaraldehyde supplemented with 4.5% sucrose, pH 7.4. After extensive washing with PBS, the cells were incubated for 10 min in 300 mM glycine in PBS, pH 10.0, and washed in 100 mM Tris-HCl, pH 7.6. The cells were then incubated for 45 min at room temperature in 1 mg/ml diaminobenzidine in freshly prepared 50 mM Tris-HCl, pH 7.6, and 0.015% H₂O₂. The cells were washed in 100 mM Tris-HCl, pH 7.6, followed by several washes with PBS, post-fixed in 75 mM cacodylate buffered 1% osmium tetroxide, and processed for electron microscopy as described above. Controls included incubation without the primary antibody and preadsorption of primary antibody with antigen.
   Immunogold. Cells were fixed as described above for the immunoperoxidase labeling, then partially dehydrated in a graded series of ethanol (70,

80, and 95%) at 0°C and infiltrated overnight at −20°C in 100% Lowicryl (2.7 gm crosslinker A, 17.3 gm crosslinker B and 0.1 gm initiator C). The Lowicryl was polymerized at ∼−40°C in a CO_2 atmosphere by U.V. radiation. The polymerized Lowicryl was removed from the glass coverslip by immersion in liquid N_2. Small pieces of polymerized Lowicryl were glued to blank Epon blocks. Thin sections were recovered on gold grids incubated with PBS containing 1 mg/ml BSA for 30 min and then labeled for 60 min at 25°C with primary antibody (affinity purified rabbit anti-PLA$_2$ antibody [20 μg/ml], mouse anti-*ras* monoclonal antibody [10 μg/ml], or rabbit anti-Na,K-ATPase antiserum [1:400 dilution]) diluted in PBS/BSA. Similar labeling efficiency was obtained by incubating sections with primary antibodies for longer intervals (up to 12 h). The sections were washed for 1 h in PBS, and labeled for 30 min at 25°C with the second antibody, either goat anti-rabbit or goat anti-mouse attached to 20- or 5-nm gold particles, respectively (Janssen Pharmaceutica, Beerse, Belgium) diluted 1:20 in PBS/BSA. The sections were then washed with numerous changes of PBS, post-fixed for 5 min in 75 mM cacodylate buffered 2% glutaraldehyde supplemented with 4.5% sucrose, pH 7.4, washed in distilled water, and air dried. Electron micrographs were taken on a Philips 201 at 60 kV. Controls included incubation without the primary antibody, preadsorption of primary antibody with antisera, and incubation with a mouse anti-HSP-72 antibody kindly provided by W. Welch (Cold Spring Harbor Laboratory, Cold Spring Harbor, NY) as a primary antibody.

Results

Antibody Characterization

Antiserum raised in rabbits against pancreatic phospholipase A$_2$ (PLA$_2$) was tested for specificity by immunoblotting analysis (Fig. 1). The antiserum was capable of detecting as little as 10 ng of purified PLA$_2$ (Fig. 1 *d*). In immunoblots of extracts from normal (NRK) and *ras*-transformed (KNRK) cells, this antiserum recognized a single 16-kD polypeptide with the same gel mobility as purified PLA$_2$ (Fig. 1, *e* and *f*). This immunoreactivity was eliminated by preadsorption of the antiserum with purified PLA$_2$ (Fig. 1, *g* and *h*). To purify the specific anti-PLA$_2$ antibodies, the serum was processed by affinity chromatography using immobilized PLA$_2$. The resulting affinity-purified antibodies recognized the 16-kD polypeptide in immunoblots of NRK and KNRK cells (Fig. 1, *i* and *j*). To further establish the specificity of the anti-PLA$_2$ antibody, we examined the effect of this antibody on the activity of cellular PLA$_2$. For this, NRK cells were grown in the presence of ^{32}P to radioactively label the phospholipids. Membranes were prepared from the radiolabeled cells, and the activity of PLA$_2$ in these isolated membranes was assayed by monitoring the time-dependent formation of two of the products of PLA$_2$ activity: lysophosphatidylcholine (lyso PC) (produced from phosphatidylcholine [PC]) and lysophosphatidylethanolamine (lyso PE) (produced from phosphatidylethanolamine [PE]). Under the conditions used in this assay, the activity of PLA$_2$ was time, temperature and calcium dependent (not shown). PE was a preferred substrate for the observed PLA$_2$ activity as evident by the higher rate of production of lyso PE as compared to lyso PC (Fig. 2, lane *1*). The accumulation of lyso PE and lyso PC was significantly inhibited when membranes were incubated with anti-PLA$_2$ antibody (Fig. 2, lane *2*). A similar degree of inhibition was detected when the anti-PLA$_2$ antibody was incubated with membranes in the presence of 10% FCS (not shown). The addition of 10% serum alone to the membrane preparation (in the absence of anti-PLA$_2$ antibody) resulted in a three-fold stimulation of PLA$_2$ activity. Incubation of membranes with IgG prepared from non-immune serum had no apparent effect on the
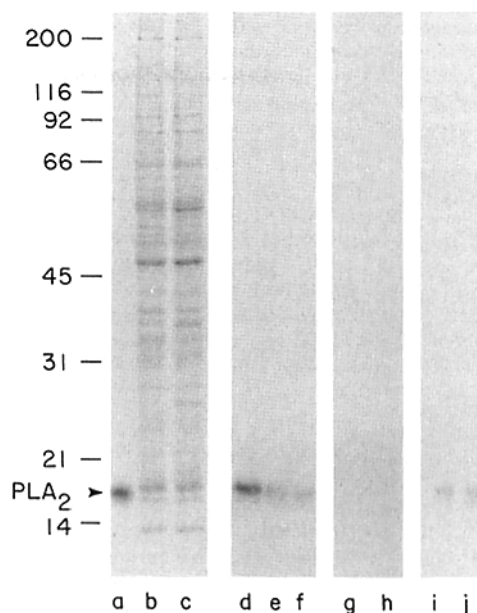

Figure 1. Detection of immunoreactive polypeptides in cell extracts by anti-PLA$_2$ antibodies. Purified PLA$_2$ (lane *a*, 1 μg; lane *d*, 10 ng) and extracts from NRK (lanes *b*, *e*, *g*, and *i*) and KNRK (lanes *c*, *f*, *h*, and *j*) cells (dissolved in SDS sample buffer) were subjected to SDS-PAGE on a 12.5% gel. After electrophoresis the proteins were either stained with Coomassie brilliant blue (lanes *a*–*c*) or electrotransferred to nitrocellulose strips (lanes *d*–*j*) for immunoblotting with anti-PLA$_2$ antibodies (immune serum (lanes *d*–*f*); immune serum preabsorbed with an excess of purified PLA$_2$, lanes *g* and *h*; affinity purified anti-PLA$_2$ IgG, lanes *i* and *j*). HRP-conjugated goat anti-rabbit antibodies were used for visualization of the immunocomplexes. The positions of molecular mass markers (kD) are indicated on the left.

production of lysophosphoglycerides (Fig. 2, lane 3). Therefore, the inhibitory effect of anti-PLA$_2$ antibody on PLA$_2$ activity most probably reflects the specific interaction of the antibody with some form(s) of membrane-bound PLA$_2$.

Immunohistochemical Localization of PLA$_2$

The affinity purified anti-PLA$_2$ antibody was used in indirect immunofluorescence experiments to localize PLA$_2$ in NRK cells. As seen in Fig. 3 *a*, the fluorescent staining was diffusely distributed throughout the cells, consistent with the biochemical localization of PLA$_2$ to virtually all subcellular membranes (Van den Bosch, 1980). A prominent feature of the immunofluorescent staining pattern was the intense staining detected in membrane ruffles (Fig. 3 *a*). This labeling pattern may indicate that PLA$_2$ is preferentially concentrated in these membranous structures. A similar PLA$_2$ distribution pattern consisting of diffuse cytoplasmic staining and intense ruffle staining was detected in several other cell types including rat embryo fibroblasts and human fibroblasts (not shown). To determine whether PLA$_2$ can be detected on the cell surface, anti-PLA$_2$ antibodies were applied to fixed NRK cells without prior permeabilization. As seen in Fig. 3 *c*, surface immunofluorescence with punctate distribution was readily visible, apparently indicating the presence of PLA$_2$ on the outer cell surface. Immunofluorescence staining of living cells with anti-PLA$_2$ antibodies similarly
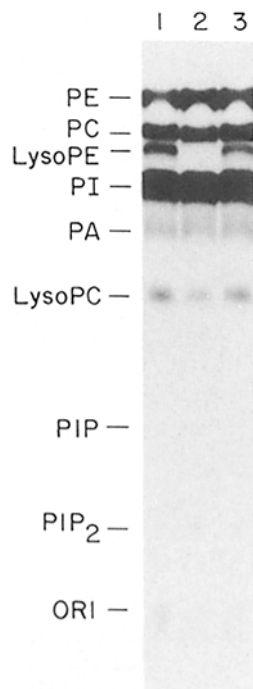
1 2 3

PE —
PC —
LysoPE —
PI —

PA —

LysoPC —

PIP —

PIP$_2$ —

ORI —

Figure 2. Effect of anti–PLA$_2$ antibodies on the activity of membrane-associated PLA$_2$. Crude membranes were prepared from ^{32}P-labeled NRK cells by hypotonic lysis and differential centrifugation. The membrane pellet was resuspended to a protein concentration of 0.2 mg/ml. Equal aliquots of the membrane suspension (100 µl) were preincubated for 2 h at 4°C after the addition of buffer (lane *1*), anti–PLA$_2$ IgG (5 µg) (lane *2*), or control IgG (10 µg) (lane *3*). The reaction mixtures were then incubated for 15 min at 37°C. A mixture of methanol/chloroform/HCl (2:1: 0.02 vol/vol/vol) was added to quench the reactions and the phospholipids were extracted, separated by thin-layer chromatography, and visualized by autoradiography as described in Materials and Methods. The positions of phospholipid standards are marked on the left margin: (*PE*) phosphatidylethanolamine; (*PC*) phosphatidylcholine; (*Lyso PE*) lysophosphatidylethanolamine; (*PI*) phosphatidylinositol; (*PA*) phosphatidic acid; (*Lyso PC*) lysophosphatidylcholine; (*PIP*) phosphatidylinositol phosphate; (*PIP$_2$*) phosphatidylinositol-bis-phosphate; (*ORI*) origin.

exhibited labeling of the outer cell surface (not shown). Comparable levels of cell surface labeling of PLA$_2$ were observed in dense and sparse cultures. In addition, extensive washing of cells for prolonged periods before labeling did not alter the intensity of cell surface labeling. Therefore, the occurrence of PLA$_2$ immunolabeling on the cell surface most probably did not reflect the adherence to the cell surface of extracellular enzyme molecules. Adsorption of anti–PLA$_2$ antibodies with purified PLA$_2$ eliminated the specific antibody staining (Fig. 3 *e*).

The cellular distribution of PLA$_2$ in transformed cells was examined using NRK cells transformed by the *ras* oncogene of Kirsten sarcoma virus (KNRK). The KNRK cells exhibit pronounced ruffling activity as well as extensive microvillar structures as detected by scanning electron microscopy (Fig. 4 *a*) or transmission electron microscopy (Fig. 4 *b*). The immunofluorescence staining pattern of PLA$_2$ in *ras*-transformed cells (Fig. 4 *c*) resembled that observed in their normal counterparts (Fig. 3 *a*) and included diffuse cytoplasmic staining and enhanced staining in membrane ruffles. Because ruffles are comprised of numerous membrane folds, the increase in the intensity of the fluorescence signal emitted from the ruffles could reflect an apparent increase in

membrane thickness. The inset in Fig. 4 *d* shows the immunofluorescent staining pattern of another membrane-associated protein, Na,K-ATPase, in KNRK cells as detected by an anti–Na,K-ATPase antibody (Sweadner and Gilkeson, 1985). The staining was found to be evenly distributed along the cell periphery and no enhanced staining was detected in the ruffles. Thus the preferential staining of membrane ruffles detected by the anti–PLA$_2$ antibody appears to be a specific feature of the cellular distribution of this antigen. The cellular distribution of PLA$_2$ was analyzed at the electron microscopic level by the indirect immunoperoxidase procedure using KNRK cells. As shown in Fig. 5 *a*, the membrane ruffles displayed a significant concentration of peroxidase reaction product compared with intracellular regions of the cell. When the anti–PLA$_2$ antibody was preadsorbed with purified PLA$_2$, no peroxidase staining was detected in ruffles (Fig. 5 *b*) as well as in other cellular regions. The presence of high concentration of PLA$_2$ in membrane ruffles did not result from the unique surface properties of the transformed KNRK cells. A similar peroxidase labeling was detected in the ruffles of the nontransformed NRK cells (not shown), consistent with the immunofluorescence data. Peroxidase reaction product was also present in some of the surface microvilli and occasionally in association with cytoplasmic vesicles (Fig. 5 *a*).

Spatial Relationship between Cellular PLA$_2$ and the ras Oncogene Protein

In previous immunofluorescence studies, the *ras* protein has been found to be uniformly distributed at the inner surface of the plasma membrane (Willingham et al., 1980; Furth et al., 1982). In addition, ultrastructural studies have indicated an increased accumulation of the *ras* protein in interdigitating microvillar structures (Willingham et al., 1980). In a recent immunofluorescent study (Myrdal and Auersperg, 1985), the *ras* oncogene protein has been shown to accumulate preferentially in membrane ruffles in KNRK cells. We have examined the spatial relationship between the *ras* oncogene protein and PLA$_2$ in the ruffles of KNRK cells, using a double immunogold labeling technique. As shown in Fig. 6 *a*, the 20 nm gold particles associated with PLA$_2$ were often identified in a form of a small individual aggregates. The distribution of the *ras* oncogene protein, specified by the smaller 5-nm gold particles, appeared to be more scattered. Furthermore, the majority of the 20-nm particle aggregates colocalized reproducibly with clusters of 5 nm gold particles (Fig. 6 *c*). Simultaneous or sequential additions of primary antibodies resulted in essentially identical distribution patterns. Likewise, reversing the gold label (20-nm gold particles for *ras* and 5-nm gold particles for PLA$_2$) had no apparent effect on the labeling pattern. The higher intensity of *ras* labeling compared with that of PLA$_2$

Figure 3. Localization of cellular PLA$_2$ by immunofluorescence. NRK cells grown on glass coverslips were fixed in 3.7% formaldehyde and permeabilized by brief extraction with 0.2% Triton X-100 in PBS (*a*, *b*, *e*, and *f*). For the detection of cell surface PLA$_2$, cells were fixed in formaldehyde (3.7%) and the permeabilization step was omitted (*c* and *d*). The cells were stained with affinity purified anti–PLA$_2$ antibodies (*a–d*) or with anti–PLA$_2$ antibodies that had been preadsorbed with an excess of purified PLA$_2$ (*e* and *f*), followed by fluorescein-conjugated goat anti–rabbit IgG. Note the intense staining in membrane ruffles (*arrows* in *a*). (*d*) The microscope was focused on the dorsal surface of the cells. Note the punctate appearance of the surface immunofluorescence of these cells. Fluorescence micrographs are shown in panels *a*, *c*, and *e*, and the corresponding phase-contrast micrographs are shown in *b*, *d*, and *f*, respectively. Bar, 20 µm.
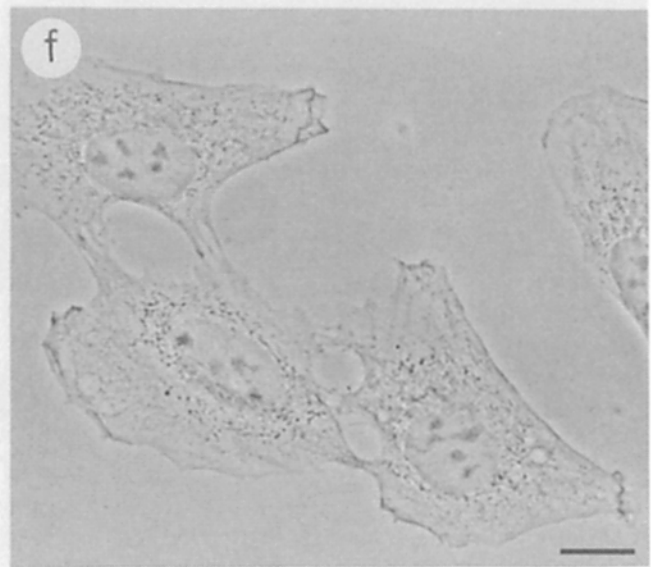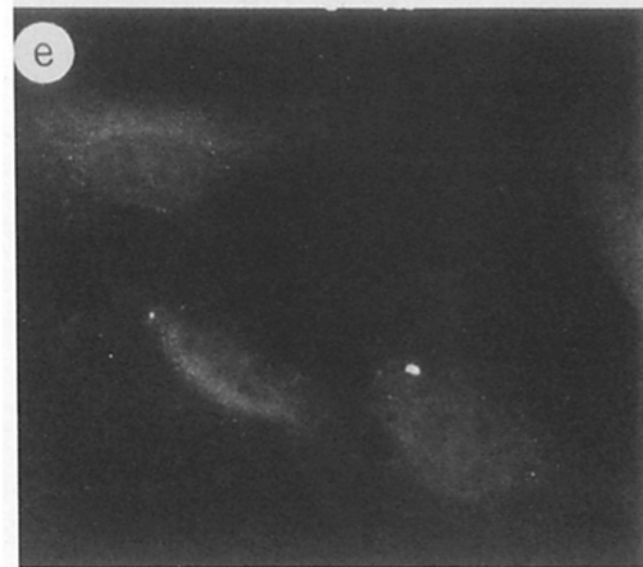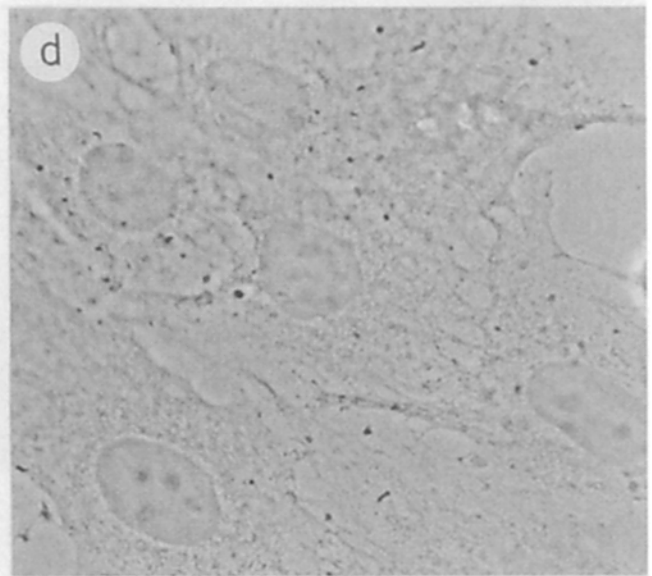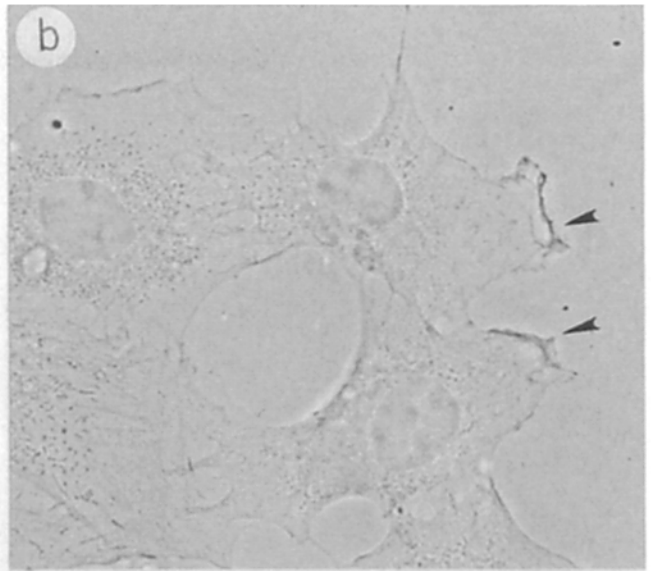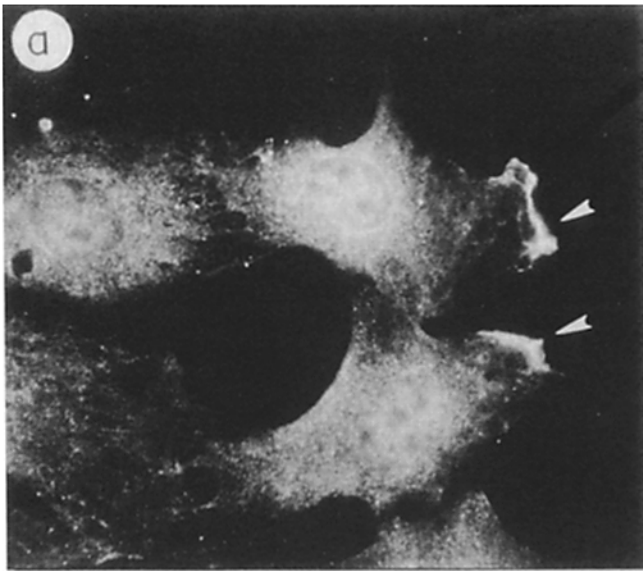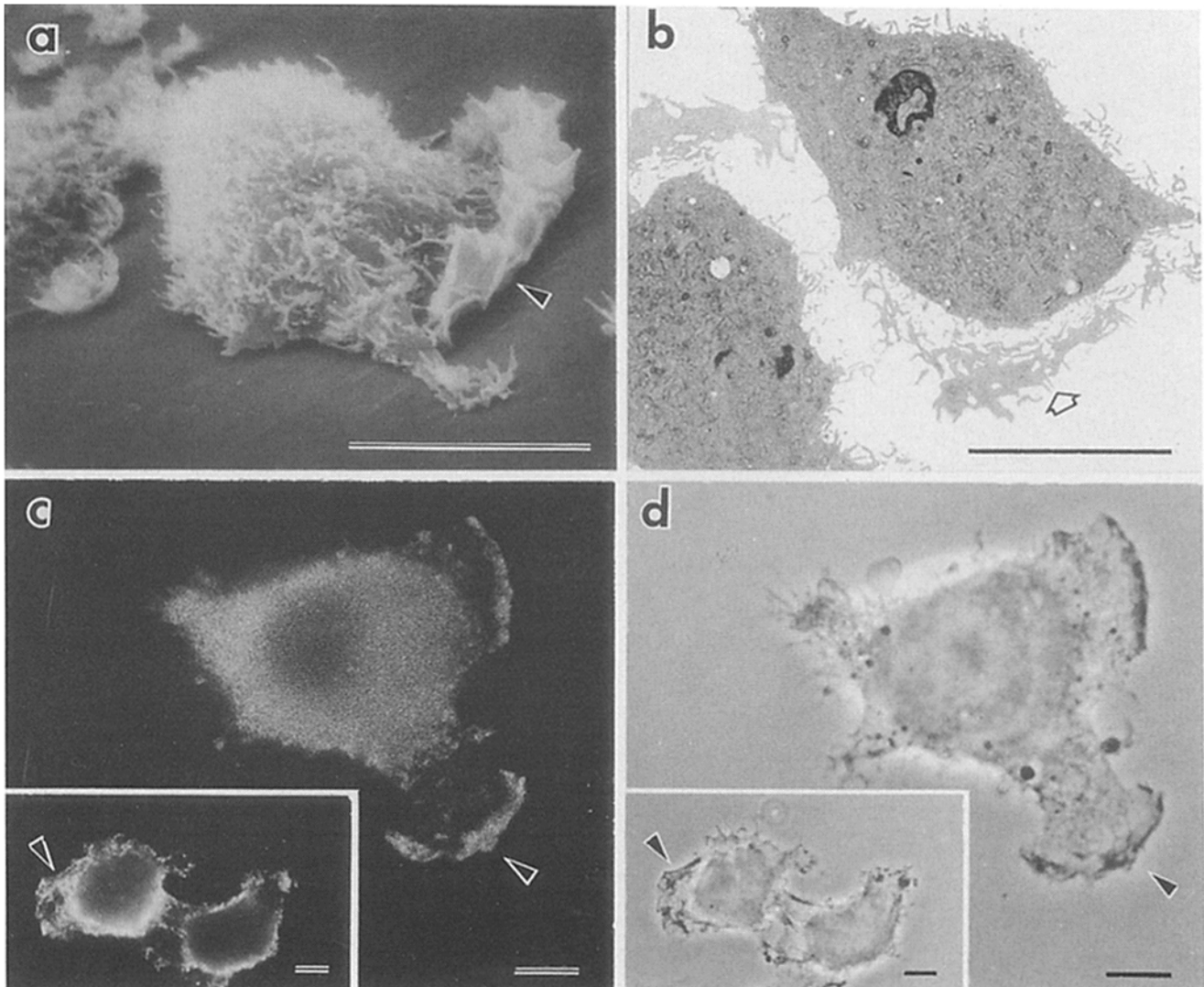
Figure 4. Surface morphology and immunofluorescence staining of KNRK cells. KNRK cells were fixed and processed for scanning electron microscopy (*a*) or for thin section transmission electron microscopy (*b*) as described in Materials and Methods. (*a*) Note the numerous surface ruffles (*arrows*) and the microvilli on the dorsal surface of the cells. (*b*) *En face* section of KNRK cells showing the ruffles (*arrow*) and a large number of short surface extensions (microvilli). Immunofluorescence staining of KNRK cells with anti-PLA$_2$ antibody (*c* and *d*) or with anti-Na,K-ATPase (*insets* in *c* and *d*) was carried out as described in the legend to Fig. 3. Note the enhanced staining of PLA$_2$ in the ruffle of KNRK cells (*arrowhead* in *c*) and the lack of preferential ruffle staining of Na,K-ATPase (*arrowhead* in *c, inset*). Fluorescence micrographs are shown in *c* and *c, inset*, and the corresponding phase-contrast micrographs are shown in *d* and *d, inset*, respectively. Bars (*a* and *b*), 20 μm; (*c* and *d*), 10 μm; (*c* and *d, insets*), 10 μm.

most probably reflected the relatively high level of expression of the *ras* oncogene protein in the virally transformed KNRK cells. On the other hand, because the intensity of immunolabeling depends on the accessibility of the specific epitopes to the antibodies, the quantitative difference in staining intensity may be apparent and could reflect a difference in the labeling efficiency between the two antigens. Considering the intrinsic resolution of the double immunogold labeling (two layers of antibodies plus gold) and

taking into account the fact that tangential sectioning of the convoluted membrane surface of the ruffle can add apparent distance between the two antigens, our observations indicate a spatial proximity between *ras* oncogene protein and PLA$_2$ within the ruffles of KNRK cells.

To further investigate the specificity of the double immunogold staining pattern, we have used the same labeling technique to examine the relationship between the distribution of the *ras* oncogene protein and another membrane protein,

---

Figure 5. Immunoperoxidase localization of PLA$_2$ in KNRK cells. Cells were fixed and processed for immunoperoxidase staining as described in Materials and Methods. (*a*) Prominent staining of the membrane ruffle in KNRK cells; (*b*) control staining using anti-PLA$_2$ antibody preadsorbed with excess purified PLA2; arrowheads in *a* and *b* point to membrane ruffles; (*a, inset*) specific staining associated with intracellular vesicles. Bars (*a* and *b*), 5 μm; (*a, inset*), 0.5 μm.

1656
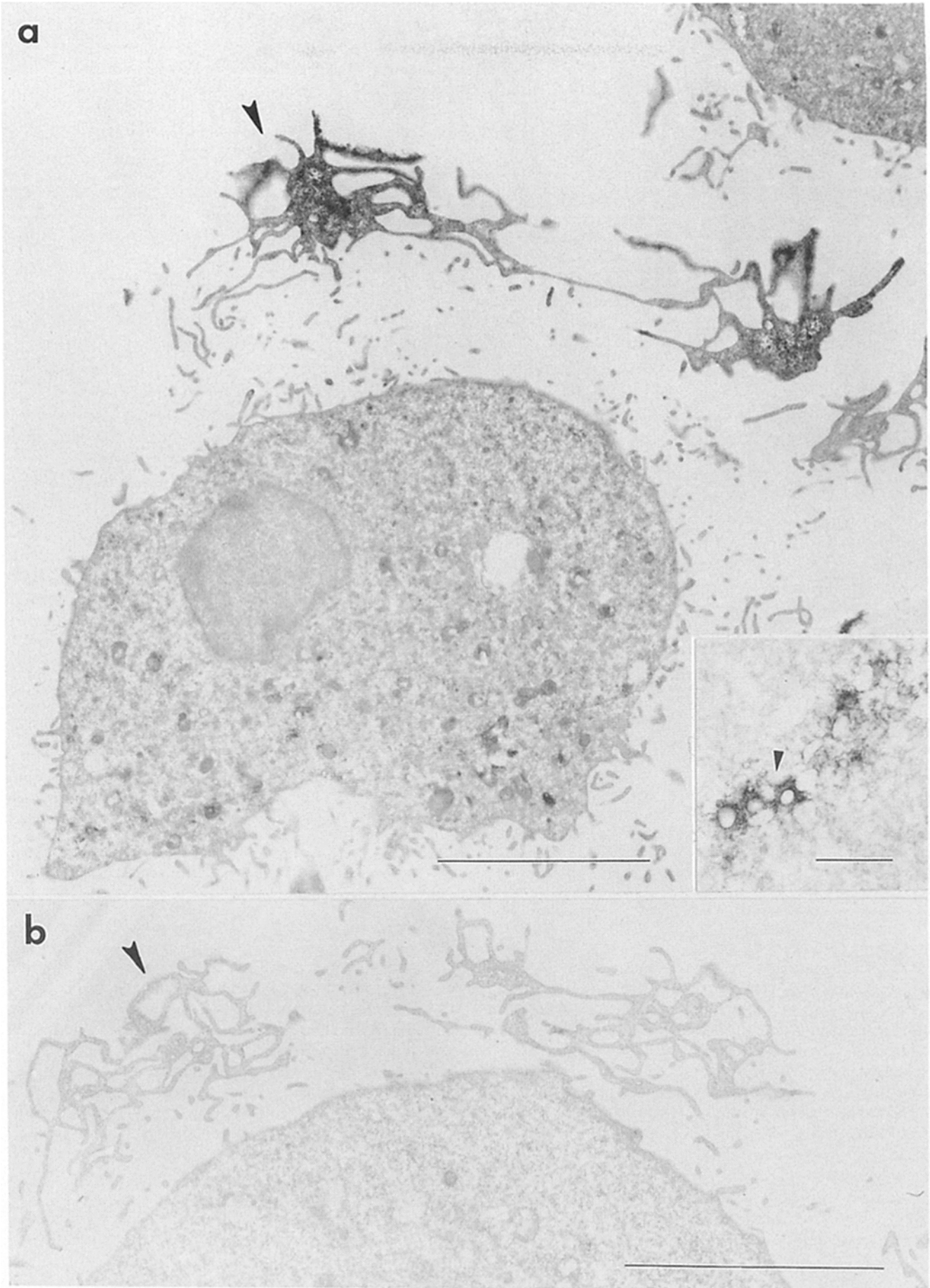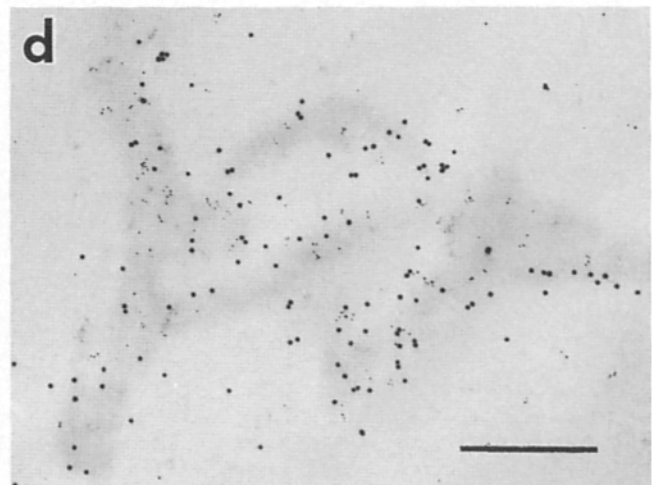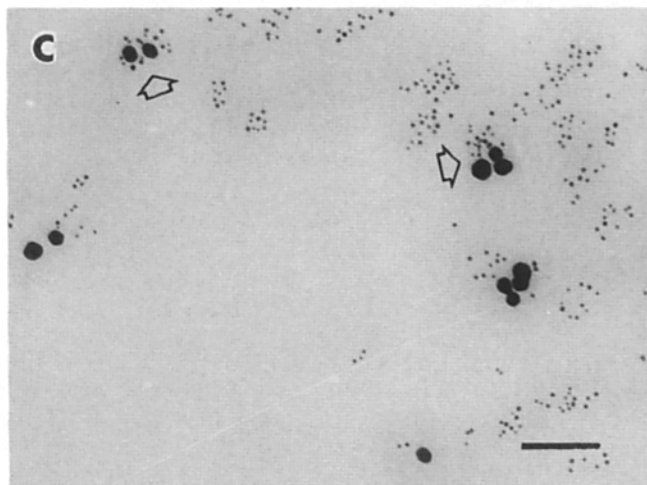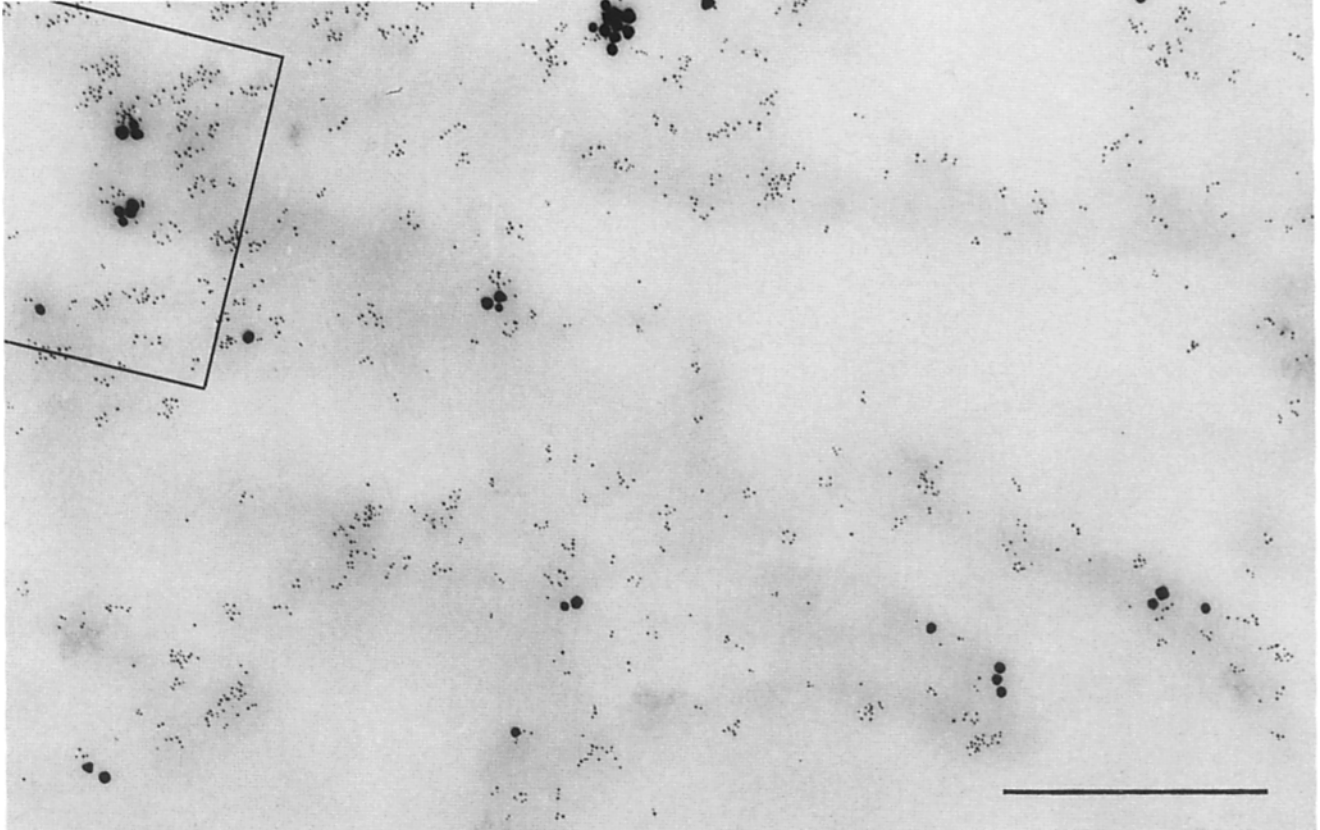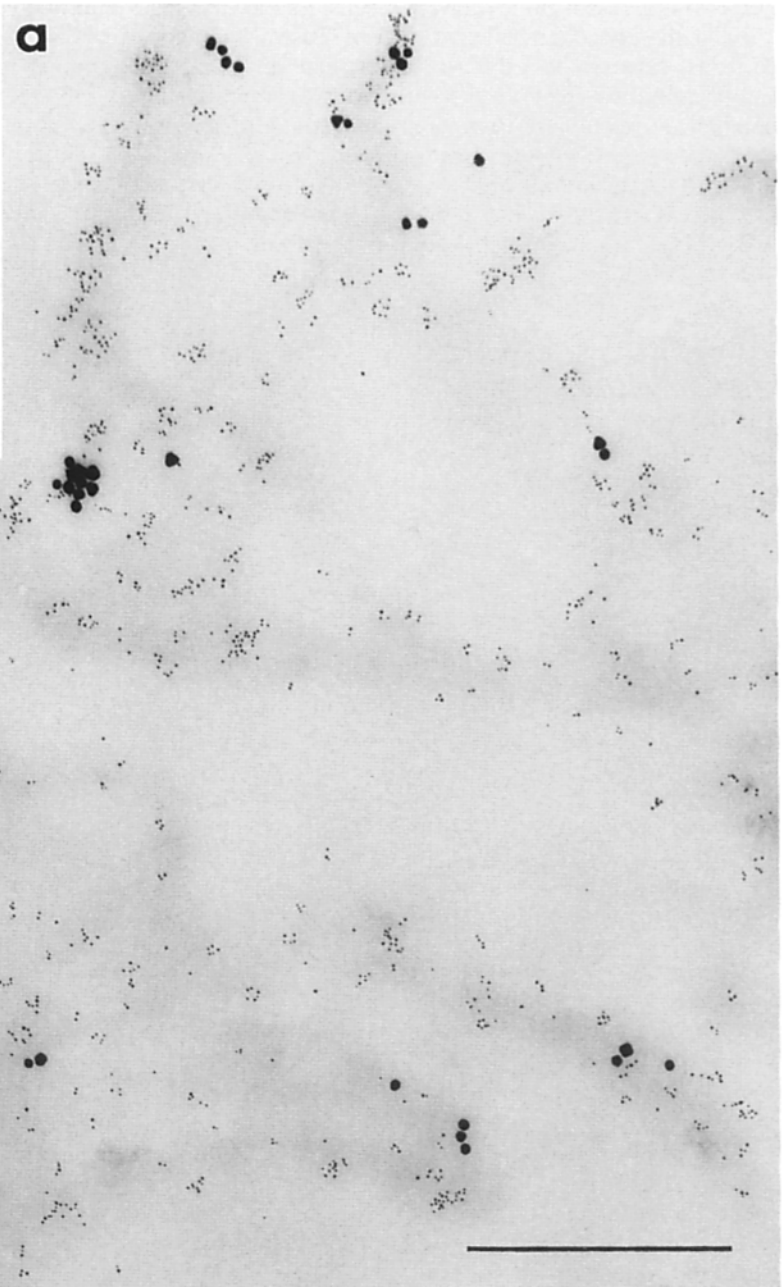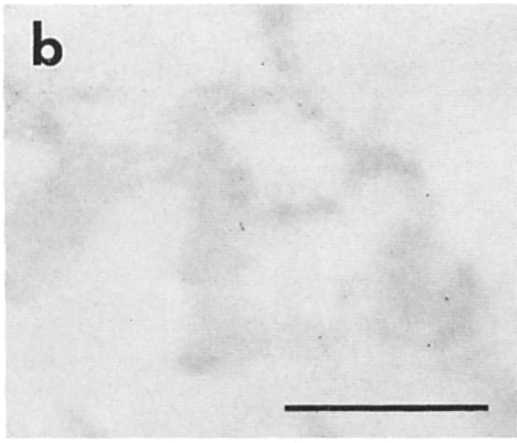
Na,K-ATPase, in the ruffles of KNRK cells. As shown in Fig. 6 d, the immunogold labeling of Na,K-ATPase (20-nm gold particles) gave rise to a diffuse staining pattern which was appreciably different from the clustered appearance of the immunogold staining of PLA$_2$ (Fig. 6 a, 20-nm gold particles). Moreover, the spatial relationship between the immunogold staining patterns of the *ras* oncogene protein (5-nm gold particles) and the Na,K-ATPase (20-nm gold particles) differed significantly from that observed between the *ras* oncogene protein and PLA$_2$.

Discussion

In this paper we describe the cellular topology of the enzyme PLA$_2$ in normal and *ras*-transformed cells and provide evidence consistent with an elevated concentration of the enzyme in membrane ruffles. We have used an anti-PLA$_2$ antibody which was generated against porcine pancreatic PLA$_2$. This antibody was immunoreactive in rat fibroblasts and exhibited an inhibitory effect on the activity of membrane-bound PLA$_2$. In agreement with previous reports (Okamoto et al., 1985; Masliah et al., 1987), our findings indicate an antigenic relatedness between an extracellular PLA$_2$ and cellular PLA$_2$ from two different mammalian species and cell types. Cellular PLA$_2$ has been shown to exist in several forms which differ from each other in their substrate specificity, calcium requirements, kinetic properties and cellular distribution (Van den Bosch, 1980; Verheij et al., 1981). The characteristics of the cellular forms of PLA$_2$ which are recognized by the anti-PLA$_2$ antibody used in this study have not been as yet determined. However, the ability of the anti-PLA$_2$ antibody to inhibit both basal and serum-stimulated PLA$_2$ activities suggests that the immunoreactive species represent at least certain forms of both the constitutive and regulated PLA$_2$. Moreover, the inhibitory effect of the anti-PLA$_2$ antibody on serum-stimulated PLA$_2$ activity indicates that the antibody can detect PLA$_2$ forms that may be functionally relevant to mitogenic signalling.

The functional significance of the presence of PLA$_2$ in the ruffles can only be speculated upon since the molecular events that regulate the process of ruffle formation are as yet not well understood. It has been shown previously that the partitioning of cis-unsaturated fatty acids (oleic, linoleic, arachidonic) into the surface membranes results in large changes in the organization of several cytoskeletal components including actin, alpha-actinin and myosin (Hoover et al., 1981). Based on these observations it has been suggested that the free fatty acids, by altering membrane lipid structure, perturb the linkage between the cytoskeleton and the membrane (Karnovsky et al., 1982). The dynamic process of ruffle formation has been shown to be accompanied by the disassembly of stress fibers, the depletion of alpha-actinin from adhesion plaques and stress fibers, and the accumulation of actin, alpha-actinin, myosin, and tropomyosin in the ruffle (Boschek et al., 1981; Meigs and Wang, 1986). The apparent parallelism between the alterations in cytoskeletal organization associated with membrane ruffling and those induced by free fatty acids, taken together with the fact that free fatty acids are a product of PLA$_2$ activity, may indicate that the accumulation of PLA$_2$ in the ruffles reflects the regulatory role of the enzyme in the sequence of events leading to the formation and maintenance of ruffles. Furthermore, the heterogeneous distribution of PLA$_2$ could provide the means by which alterations of membrane structure due to the enzymatic activity of the protein can be produced in a localized, site-specific manner.

The occurrence of PLA$_2$ on the cell surface as detected by immunofluorescence staining is consistent with a previous report showing that the membrane associated PLA$_2$ from sheep erythrocytes is oriented towards the exterior of the cell (Frei and Zahler, 1979). The distinction between the role of cell surface PLA$_2$ and intracellular membrane-associated PLA$_2$, if such a distinction exists, is not clear. It is possible that the presence of PLA$_2$ on the cell surface represents a functional aspect of the catalytic activity of the enzyme and corresponds to the asymmetric distribution and the transmembrane movement of the enzyme's substrates, the phosphoglycerides. Alternatively, since several mammalian tissues contain a secretory form of PLA$_2$ (Verheij et al., 1981) which appears to be immunochemically related to the intracellular form (Okamoto et al., 1985), the immunoreactivity detected on the outer cell surface may correspond to the enzyme molecules that are undergoing secretion.

A large number of observations made over the past decade have contributed to the realization that cell surface morphology and its dynamic alterations are invariable correlates of cell proliferation. The causal association between plasma membrane motility and the proliferative capacity of cells, however, is unknown. NRK cells transformed by the v-K-*ras* oncogene (KNRK) show an enhanced and continuous membrane ruffling activity compared with normal NRK cells (Myrdal and Auersperg, 1986). This enhanced ruffling activity appears to be linked to the cellular function of the *ras* oncogene protein since microinjection of anti-*ras* antibodies into KNRK cells diminishes significantly membrane ruffling (Bar-Sagi et al., 1987). The cellular distribution of PLA$_2$ in *ras*-transformed cells resembles that observed in normal cells in that the enzyme is diffusely distributed within cellular membranes and is concentrated under ruffles. This distribution pattern resembles that displayed by the K-*ras* oncogene protein. Specifically, both proteins accumulate preferentially in membrane regions that show intense ruffling activity.

Figure 6. Double-immunogold labeling of PLA$_2$ and the *ras* protein in the membrane ruffles of KNRK cells. Thin sections of surface ruffles were simultaneously stained with affinity purified rabbit anti-PLA$_2$ antibodies and mouse monoclonal anti-*ras* IgG (*a*). For controls, these antibodies were first preabsorbed with an excess of purified PLA$_2$ and the *ras* protein, respectively (*b*). *d* Shows another example of double immunogold staining of ruffles using rabbit anti-Na,K-ATPase and mouse monoclonal anti-*ras* IgG. The sections were incubated with gold-conjugated (20-nm particles) goat anti-rabbit IgG and gold-conjugated (5-nm particles) goat anti-mouse IgG. The ruffles which appear as the darker grey regions of the electron micrographs have a characteristic convoluted appearance. Staining of the sections with heavy metals was avoided to allow for the unobstructed visualization of the small gold particles. The area marked by the box in *a* is shown in higher magnification in *c*. Note the colocalization of the PLA$_2$ immunogold labeling with the *ras* immunogold labeling (arrows). Bars (*a* and *b*), 0.5 µm; (*c*), 0.1 µm; (*d*), 0.5 µm.

Analysis of the spatial relationship between PLA$_2$ and the K-*ras* oncogene protein, carried out at a high level of resolution by the use of the double immunogold labeling method, reveals a close proximity (∼100–500 Å) between PLA$_2$ immunoreactive labeling and the *ras* oncogene protein in the ruffles. Since the double labeling pattern of the *ras* oncogene protein and another membrane protein, the Na,K-ATPase, had different characteristics, the proximity between the immunogold staining of the *ras* oncogene protein and PLA$_2$ cannot be attributed solely to the occurrence of the two antigens in the same subcellular compartment. The large excess of the *ras* immunogold labeling over the PLA$_2$ immunogold labeling makes it difficult to assess quantitatively the co-localization pattern. Nevertheless, we have estimated that on the average the surface area that is occupied by the *ras*-associated gold particles is ∼50% of the total surface area of the ruffle. Since the proportion of PLA$_2$-associated gold particles which are found in close proximity to the *ras*-associated gold particle is significantly higher (∼85%), the colocalization of the two antigens most probably reflects their spatial relatedness. Since little is known as yet about the mechanisms by which the cellular activities of PLA$_2$ and the *ras* protein are controlled, it is difficult to assess the extent to which the coincident subcellular location of these two proteins reflects a functional relationship. In this context it is interesting, however, to note that microinjection of the *ras* oncogene protein into quiescent fibroblasts results in a time-dependent stimulation of PLA$_2$ activity (Bar-Sagi and Feramisco, 1986). In addition, we have found that the steady-state levels of PLA$_2$ activity are significantly higher in *ras*-transformed NRK cells as compared to normal NRK cells (Bar-Sagi, D., and J. R. Feramisco, unpublished observations). Lastly, pertussis toxin sensitive GTP-binding proteins have been recently implicated in the coupling of certain types of receptors to PLA$_2$ activation (Bokoch and Gilman, 1984; Burch et al., 1986). Thus, the apparent similarities in the distribution patterns of the *ras* oncogene protein and PLA$_2$ shown here suggest the possibility that the two proteins may act within the same regulatory pathway.

References

Bar-Sagi, D., and J. R. Feramisco. 1986. Induction of membrane ruffling and fluid-phase pinocytosis in quiescent fibroblasts by *ras* proteins. *Science (Wash. DC).* 233:1061–1068.

Bar-Sagi, D., F. McCormick, and J. R. Feramisco. 1987. Inhibition of cell surface ruffling and fluid-phase pinocytosis by microinjection of anti-*ras* antibodies into living cells. *J. Cell Physiol.* 5:69–73.

Blattler, D. P., F. Garner, K. Van Slyke, and A. Bradley. 1972. Quantitative electrophoresis in polyacrylamide of 2–40%. *J. Chromatogr.* 64:147–155.

Bokoch, G. M., and A. G. Gilman. 1984. Inhibition of receptor-mediated release of arachidonic acid by pertussis toxin. *Cell.* 39:301–308.

Bormann, B. J., C.-K. Huang, W. M. Mackin, and E. L. Becker. 1984. Receptor-mediated activation of phospholipase A$_2$ in rabbit neutrophil plasma membrane. *Proc. Natl. Acad. Sci. USA.* 81:767–770.

Boschek, C. B., B. M. Jockusch, R. R. Friis, R. Back, E. Grundmann, and H. Bauer. 1981. Early changes in the distribution and organization of microfilament proteins during cell transformation. *Cell.* 24:175–184.

Burch, R. M., A. Luini, and J. Axelrod. 1986. Phospholipase A$_2$ and phospholipase C are activated by distinct GTP-binding proteins in response to α-adrenergic stimulation in FRTL5 thyroid cells. *Proc. Natl. Acad. Sci. USA.* 83:7201–7205.

Chang, J., S. Gilman, and A. J. Lewis. 1986. Interleukin 1 activates phospholipase A$_2$ in rabbit chondrocytes: A possible signal for IL 1 action. *J. Immunol.* 136:1283–1287.

Dinarello, C. A., S. O. Marnoy, and L. J. Rosenwasser. 1983. Role of arachidonate metabolism in the immunoregulatory function of human leukocytic pyrogen/lymphocyte-activating factor/interleukin 1. *J. Immunol.* 130:890–894.

Frei, E., and P. Zahler. 1979. Phospholipase A$_2$ from sheep erythrocyte membranes. Ca^{++} dependence and localization. *Biochim. Biophys. Acta.* 550:450–463.

Furth, M. E., L. J. Davis, B. Fleurdelys, and E. M. Scolnick. 1982. Monoclonal antibodies to the p21 products of the transforming gene of Harvey murine sarcoma virus and of the cellular *ras* gene family. *J. Virol.* 43:294–304.

Haas, G. H. de, N. M. Posteman, W. Nieuwenhuizen, and L. L. M. van deenen. 1968. Purification and properties of phospholipase A from porcine pancreas. *Biochim. Biophys. Acta.* 159:103–117.

Hoover, R. L., K. Fujiwara, R. D. Klausner, D. K. Bhalla, R. Tucker, and M. J. Karnovsky. 1981. Effect of free fatty acids on the organization of cytoskeletal elements in lymphocytes. *Mol. Cell. Biol.* 1:939–948.

Karnovsky, M. J., A. M. Kleinfeld, R. L. Hoover, and R. D. Klausner. 1982. The concept of lipid domains in membranes. *J. Cell Biol.* 94:1–6.

Laemmli, U. K. 1970. Cleavage of structural proteins during the assembly of the head of bacteriophage T4. *Nature (Lond.).* 227:680–685.

Lands, W. E. M. 1979. The biosynthesis and metabolism of prostaglandins. *Annu. Rev. Physiol.* 41:633–652.

McGrail, K. M., and K. J. Sweadner. 1986. Immunofluorescent localization of two different Na,K-ATPases in the rat retina and in identified dissociated retinal cells. *J. Neurosci.* 6:1272–1283.

McKean, M. L., J. B. Smith, and M. J. Silver. 1981. Formation of lysophosphatidylcholine by human platelets in response to thrombin. *J. Biol. Chem.* 256:1522–1524.

Masliah, J., C. Kadri, D. Pepin, T. Rybkine, J. Etienne, J. Chambaz, and G. Bereziat. 1987. Antigenic relatedness between phospholipase A$_2$ from *Naja naja* venom and from mammalian cells. *FEBS (Fed. Eur. Biol. Soc.) Lett.* 222:11–16.

Meigs, J. B., and Y. L. Wang. 1986. Reorganization of alpha-actinin and vinculin induced by a phorbol ester in living cells. *J. Cell Biol.* 102:1430–1438.

Myrdal, S. E., and N. Auersperg. 1985. p21 ras. Heterogeneous localization in transformed cells. *Exp. Cell Res.* 159:441–450.

Myrdal, S. E., and N. Auersperg. 1986. An agent or agents produced by virus transformed cells cause unregulated ruffling in untransformed cells. *J. Cell Biol.* 102:1224–1229.

Okamoto, M., T. Ono, H. Tojo, and T. Yamana. 1985. Immunochemical relatedness between secretory phospholipase A$_2$ and intracellular phospholipase A$_2$. *Biochem. Biophys. Res. Comm.* 128:788–794.

Shier, W. T., and J. P. Durkin. 1982. Role of stimulation of arachidonic acid release in the proliferative response of 3T3 mouse fibroblasts to platelet-derived growth factor. *J. Cell Physiol.* 112:171–181.

Siraganian, R. P. 1983. Histamine secretion from mast cells and basophils. *Trends Pharmacol.* 4:432–437.

Sweadner, K. J., and R. C. Gilkeson. 1985. Two isozymes of the Na,K-ATPase have distinct antigenic determinants. *J. Biol. Chem.* 254:6060–6067.

Towbin, H., T. Staehelin, and J. Gordon. 1979. Electrophoretic transfer of proteins from polyacrylamide gels to nitrocellulose sheets: procedure and some applications. *Proc. Natl. Acad. Sci. USA.* 76:4350–4354.

Van den Bosch, H. 1980. Intracellular phospholipase A. *Biochim. Biophys. Acta.* 604:191–246.

Verheij, H. M., A. J. Slotboom, and G. H. de Haas. 1981. Structure and function of phospholipase A$_2$. *Rev. Physiol. Biochem. Pharmacol.* 91:91–203.

Vicentini, L. M., R. J. Miller, and M. L. Villereal. 1984. Evidence for a role of phospholipase activity in the serum stimulation of Na$^+$ influx in human fibroblasts. *J. Biol. Chem.* 259:6912–6919.

Willingham, M. C., I. Pastan, T. C. Shih, and E. M. Scolnick. 1980. Localization of the *src* gene product of the Harvey strain of MSV to the plasma membrane of transformed cells by electron microscopic immunocytochemistry. *Cell.* 19:1005–1014.

Wong, G., N. Arnheim, R. Clark, P. McCabe, M. Innis, L. Aldwin, D. Nitecki, and F. McCormick. Detection of activated M_r 21,000 protein, the product of *ras* oncogene, using antibodies with specificity for amino acid 12. *Cancer Res.* 46:6029–6033.